Accepted Manuscript

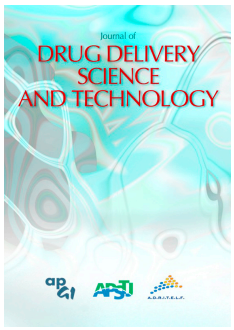

The influence of surfactant on the properties of albendazole-bile salts particles designed for lung delivery

P.M. Natalini, M.F. Razuc, J.B. Sørli, V. Bucalá, M.V. Ramírez-Rigo

PII: S1773-2247(19)30482-4

DOI: https://doi.org/10.1016/j.jddst.2019.101162

Article Number: 101162

Reference: JDDST 101162

To appear in: *Journal of Drug Delivery Science and Technology*

Received Date: 5 April 2019

Revised Date: 26 June 2019

Accepted Date: 16 July 2019

Please cite this article as: P.M. Natalini, M.F. Razuc, J.B. Sørli, V. Bucalá, M.V. Ramírez-Rigo, The influence of surfactant on the properties of albendazole-bile salts particles designed for lung delivery, *Journal of Drug Delivery Science and Technology* (2019), doi: https://doi.org/10.1016/j.jddst.2019.101162.

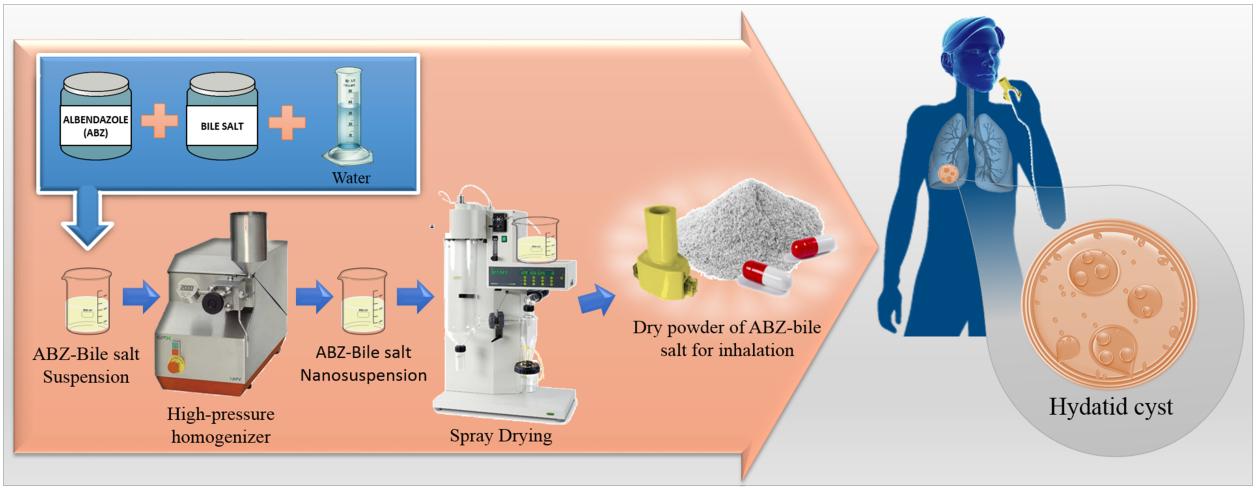

THE INFLUENCE OF SURFACTANT ON THE PROPERTIES OF ALBENDAZOLE-BILE SALTS PARTICLES DESIGNED FOR LUNG DELIVERY

Natalini, P.M.[1, 2, 5]; Razuc, M.F.[1, 2*]; Sørli, J. B.[3]; Bucalá, V.[2, 4]; Ramírez-Rigo, M.V.[1, 2]

[1]Departamento de Biología, Bioquímica y Farmacia. Universidad Nacional del Sur (UNS). Bahía Blanca, Argentina.

[2]Planta Piloto de Ingeniería Química (PLAPIQUI), UNS- CONICET. Bahía Blanca, Argentina.

[3]The National Research Centre for the Working Environment. Copenhagen, Denmark.

[4]Departamento de Ingeniería Química, UNS. Bahía Blanca, Argentina.

*Corresponding author. Camino La Carrindanga Km 7 - C. C. 717 - 8000 Bahía Blanca. Argentina. Tel.: +54-(0)291-4861700. Fax: +54-(0)291-4861600. email: mariela.razuc@uns.edu.ar

[5] Present address: University of Southern Denmark (SDU). 305 Memphys. Campusvej 55 5230 Odense M, Denmark.

Abstract

Albendazole is a first line drug for the treatment of several parasitic diseases in humans. Some parasites target the lungs, however lung delivery of albendazole has so far not been reported. We have developed albendazole-based powders suitable for pulmonary delivery, and studied the impact of surfactant on the formulation properties. High-pressure homogenization followed by spray drying was used to produce inhalable particles of albendazole containing the bile salts sodium taurocholate and sodium glycocholate. The process resulted in porous microparticles, that exhibited good spray drying yield (> 50%), low moisture contents (< 1%) and aerodynamic D_{90} < 5 µm. The particles showed adequate aerosolization performance either for normal conditions (respiratory fraction > 71%) or conditions that simulate decreased respiratory capacity (respiratory fraction > 49%). The powders did not disturb lung surfactant function. The comparison between both formulations has revealed that the properties of the surfactants affect mainly the particle size of the suspensions and the porosity of the powders. The higher porosity of the albendazole-sodium taurocholate powder led to an enhanced aerodynamic performance of the formulation compared to albendazole-sodium glycocholate. The developed albendazole powders may pave a way for local lung treatment of parasitic diseases.

Keywords

Nanoaggregates; high-pressure homogenization; spray drying; sodium taurocholate; sodium glycocholate, dry powder inhaler.

1. Introduction

Hydatidosis or human cystic echinococcosis (CE) is a cosmopolitan zoonotic disease that can be found in people and livestock infected with the larval stage of the nematode *Echinococcus granulosus* [1]. In humans, the outcome of this infection is cyst development in different organ systems, with the liver (65%) and the lungs (25%) being the most commonly affected organs [2, 3]. Since lungs have high elasticity, pulmonary cysts grow very fast [4].

Albendazole (ABZ) is the drug of choice for chemotherapeutic treatment of CE [5, 6]. It is known that the success of the chemotherapeutic treatment of CE depends on the capacity of the drug to access to the hydatid cyst at adequate concentrations for sufficient periods of time [7]. Since drugs administered by the oral route, once absorbed, access to the liver through the portal vein to be metabolized, this route is useful for treatment of hepatic hydatid cysts. Treatment of pulmonary CE by local administration of ABZ through the pulmonary route has so far been an unexplored alternative. There are several advantages of delivering drugs directly to the lungs, it allows the use of lower doses than those required orally, while it reduces possible side effects and, at the same time, high local concentrations are reached at the site of action [8].

Designing suitable aerosols for inhalation is challenging. Particle size is one of the most important characteristics in dry powder inhaler formulations, together with shape, porosity, density, electrical charge and hygroscopicity [9]. In order to reach the lower respiratory tract and optimize pulmonary drug deposition, the formulations need to have aerodynamic diameters between 0.5 and 5 µm [10]. Once in the respiratory parts of the lungs, particles can interact with components of the lung surfactant (LS) film and this interaction depends on the physical properties of the particles [11].

A widely used method to produce particles for pulmonary delivery is spray drying (SD) [9]. One of the main advantages of this technique is that the characteristics of the resulting particles can be controlled by adjusting the formulation and process parameters [12, 13]. This scalable technology is able to process a variety of liquids. If the water

solubility of drugs is very low preparation of solutions using organic solvents or aqueous suspensions are some of the available alternatives. The main disadvantage of organic solvents is their toxicity related to the presence of residual solvents in the final product, therefore, aqueous suspensions are preferred [9].

Since suspensions are unstable heterogeneous mixtures, they must be stabilized. One way to stabilize suspensions is by using surfactants. In the literature on pulmonary delivery, bile salts, such as salts of cholate, deoxycholate, glycocholate, glycodeoxycholate, taurocholate and taurodeoxycholate are used [14-21]. Bile salts have other important roles in drug absorption and the aerodynamic properties of powders [14]. Therefore, the selection of the surfactant is a relevant formulation factor.

During the spray drying process, solid drugs in suspension aggregate and form dried particles with a larger size than the starting material [9]. Hence, in order to obtain microparticles suitable for pulmonary deposition by SD, suspensions need to be previously processed to obtain particles in the nanometric range (e.g. by high-pressure homogenization, HPH).

As mentioned above, to date, no formulations targeting ABZ to the lung have been reported. Therefore, the present study has addressed the production, characterization and comparison of new dry powder formulations based on albendazole and two different bile salts, namely sodium taurocholate (STC) and sodium glycocholate (SGC), for pulmonary delivery. The novel formulations were obtained by processing ABZ-bile salts suspensions by high-pressure homogenization followed by spray drying. Both formulations were characterized and compared in terms of particle size, surface tension, morphology, powder density, porosity and aerodynamic properties. The effect of the ABZ-bile salt formulations on LS function was also evaluated.

The ABZ-bile salt formulations manufactured and characterized in the present article have the potential for filling the therapeutic niche of treating pulmonary parasitic diseases, such as CE.

2. Materials and methods

2.1. Materials

ABZ and lactose monohydrate (both pharmaceutical grade), as well as gelatin capsules number 3 were purchased from Saporiti (Buenos Aires, Argentina). Sieved lactose (+100 ASTM mesh) with D_{10}= 167.8 µm, D_{50}= 234.9 µm and D_{90}= 336.4 µm was used as a carrier. STC and SGC (both analytical grade), were purchased from Sigma Aldrich (St. Luis, MO, USA). Curosurf was produced by Chiesi (Parma, Italy). The unidose RS01 high resistance inhaler (Plastiape, Milano, Italy) and the multidose Turbuhaler device (AstraZeneca, Gothenburg, Sweden) were used as model inhalers. Ethyl alcohol 96% (Pharmacopoeia quality, Porta, Argentina) and bidistilled water were also used.

2.2. Characterization of the ABZ-bile salt suspensions

2.2.1. Preparation and particle size analysis of suspensions

Aqueous solutions containing either STC or SGC (0.03% w/v) were prepared. ABZ suspensions were obtained by adding ABZ (1% w/v) to the surfactant solution under magnetic stirring for 30 min. The bile salt concentration in the suspension was selected based on stability [22] and safety considerations [17, 21] (for more details, please see Section 1.S in the Supplementary material).

After dispersion, the suspensions were subjected to a first size reduction step using a PRO200 homogenizer (Tecnolab, Argentina) at 30,000 rpm (10 min for a sample of 500 mL). Then, a second reduction/deagglomeration step using sonication (Cole Parmer ultrasonic cleaner) (10 min for a sample of 500 mL, at a frequency of 40 kHz) was performed. Samples were withdrawn after each step to evaluate particle size distributions.

The particle size distributions were determined by using laser diffraction (LA 950V2, Horiba, Kyoto, Japan, Liquid method). For the measurement, 2 mL of suspensions were added to 200 mL of recirculating bidistilled water from the laser diffraction equipment.

The average size distribution was reported as median volumetric diameter (D_{50}) and the distribution width was informed as span (see Eq.1).

$$Span = \frac{D_{90} - D_{10}}{D_{50}} \quad (1)$$

In Eq. 1, D_{10}, D_{50} and D_{90} represent the diameters where the 10%, 50% and 90% of the population is below each value, respectively. Span values below 2 indicate relatively narrow distributions [23].

2.2.2. Surface tension determination

In order to analyze the effect of the type of bile salt over the surface tension of the suspensions, the surface tension of bidistilled water, STC solution (0.03% w/v), SGC solution (0.03% w/v), ABZ-STC suspension after homogenization/sonication and ABZ-SGC suspension after homogenization/sonication was determined.

The measurements were performed with a ring Krüss tensiometer (Krüss GmbH, Hamburg, Germany). All determinations were carried out in duplicate at a temperature of 20.7 ± 0.4 °C.

2.3. Preparation and particle size analysis of nanosuspensions

The suspensions were further processed by HPH technique (APV homogenizer, Soeborg, Denmark) to obtain nanosuspensions. The coarse suspensions (Section 2.2.1) were subjected to HPH for 10, 20 and 30 cycles at 800 bar. By using an external heat exchanger, the suspension temperature was maintained at around 30°C. The intensity-weighted average hydrodynamic diameter and polydispersity index (PdI) of the aqueous nanosuspensions were determined by photon correlation spectroscopy (PCS) using a Zetasizer Nano ZS (Malvern Instruments, UK). For this measurement, the nanosuspensions were diluted with bidistilled water up to an ABZ final concentration of

0.25% w/v. Mean particle diameters were reported as "Z-average" diameters. All determinations were carried out in triplicate.

2.4. Spray drying

The aqueous nanosuspensions were atomized in a lab-scale spray drier (Mini Spray Dryer B-290, BÜCHI, Flawil, Switzerland) equipped with a high performance cyclone. A two-fluid nozzle with a cap-orifice diameter of 0.5 mm was used. The nanosuspensions were spray dried under constant stirring to keep the samples homogeneous. The following conditions were used during the procedure: air inlet temperature (co-current flow): 110°C; drying air flowrate: 35 m^3/h; liquid feed flowrate: 1.5 mL/min and atomization air flowrate: 670 L/h. These conditions were selected based on preliminary studies. The process yield was calculated as the ratio of the powder weight obtained in the product collection vessel with respect to the total solids fed to the system. All determinations were carried out in duplicate.

2.5. Characterization of the SD products

2.5.1. Moisture content

The moisture content of the SD products was measured using a halogen moisture analyzer (MB45, Ohaus, Pine Brook, United States). The determination was carried out using samples of around 500 mg. They were heated up to 80°C until the weight changes were less than 1 mg in 60 s.

2.5.2. Particle size analysis

The particle size distribution (PSD) of powders obtained by spray drying (SD ABZ-STC and SD ABZ-SGC) was obtained by laser diffraction (LA 950V2, Horiba, Kyoto, Japan), using the dry powder method. Since the resulting powders were cohesive, the SD samples were dispersed in relative coarse lactose (sample:lactose =1:4) to improve the flow from the feed hopper to the measuring cell [24]. The lactose PSD did not interfere

with the PSD of the microparticles obtained by spray drying. The PSDs for ABZ and lactose were also measured in triplicate.

2.5.3. Scanning electron microscopy (SEM)

The morphology of ABZ raw material and the SD powders ABZ-STC and ABZ-SGC was analyzed by scanning electron microscopy (SEM), using a EVO 40-XVP, LEO scanning electron microscope (Oberchoken, Germany). The samples were metalized with a thin layer of gold using a sputter coater (PELCO 91000, TellPella, Canada). The scanning electron microscope was operated at an acceleration voltage of 10 kV.

2.5.4. Bulk and tap density

Bulk and tap density of ABZ raw material, SD powders (ABZ-STC and ABZ-SGC) and lactose were measured by using a 10 mL graduated cylinder. Bulk density (δ_{bulk}) was calculated as the ratio of the weight of the powder poured in the cylinder with respect to the volume occupied by the powder. Tap density (δ_{tap}) was calculated by tapping the cylinder until no measurable change in volume was observed. All determinations were made in triplicate. Carr Index (*CI*) was calculated using Eq.(2) and the results were interpreted according USP classification [25].

$$CI\ (\%) = \frac{\delta_{tap} - \delta_{bulk}}{\delta_{tap}} x\ 100 \qquad (2)$$

2.5.5. Porosity

Pore size distribution of the SD ABZ-STC and SD ABZ-SGC powders was determined in a Autosorb iQ gas sorption analyzer (Quantachrome Instruments, Boynton Beach, FL, USA) by using the Brunauer-Emmet-Teller (BET) method (relative pressure range: 0.05-0.30). Samples were degassed at 50°C for 24 h before analysis. Pore volume distribution was calculated with the Barrett-Joyner-Halenda (BJH) model.

2.5.6. Aerodynamic performance

The aerodynamic particle size distribution of SD ABZ-STC and SD ABZ-SGC powders was determined using a Next Generation Impactor (NGI, Coplay, Nottingham, UK) [26, 27] equipped with a pre-separator (PS).

To ensure an adequate dispersibility of the particles, the samples were mixed with lactose in a ratio 1:2 (SD powder:lactose w/w) and 1:1 (SD powder:lactose w/w). It is known that during inhalation, the drug particles are detached from the surface of lactose, the carrier particles impact in the oropharynx and the upper airways and they are swallowed, while the inhalable drug particles go to the lower parts of the respiratory tract [28].

A 3-size gelatin capsule was filled with 80 mg of the powder**.** The doses used represent 3.25% or 5% of the maximum dose administered orally in adults (400 mg twice per day). The filled capsule was placed in a RS01 high resistance inhaler (Plastiape). The NGI stages were precoated with glycerin to avoid particle re-entrainment.

Pressure drops of 2 and 4 kPa across the NGI were assayed, being the circulating air flowrate 42.5 and 60 L/min, respectively. Although USP specifies as a standard test condition a pressure drop of 4 kPa, the formulations have also been tested at 2 kPa to evaluate the effect of the inspiration rate on the aerosolization performance [26]. For both flowrates analyzed, the aerodynamic cutoff diameters of each stage of the NGI were calculated as previously described [25-27, 29].

The powders deposited on the NGI stages, inhaler, induction port, mouthpiece adapter and PS were recovered with an appropriate volume of ethanol. The ABZ content in each stage or NGI component was determined by UV spectrophotometry at 217 nm.

Experiments were done in triplicate. The emitted fraction (EF), the fine particle fraction (FPF) and respirable fraction (RF) were calculated as follows [30]:

$$EF\% = \frac{\text{drug mass deposited on induction port, pre-separator and all the NGI stages}}{\text{total drug recovered}} \times 100 \qquad (3)$$

$$FPF\% = \frac{\text{drug mass deposited on stages 3–7 and micro–orifice collector}}{\text{drug mass deposited on induction port, pre–separator and all the NGI stages}} \times 100 \quad (4)$$

$$RF\% = \frac{\text{drug mass deposited on stages 3–7 and micro–orifice collector}}{\text{total drug recovered}} \times 100 \quad (5)$$

The mass median aerodynamic diameter (*MMAD, D_{50}*), D_{10} and D_{90} as well as the percentage of particles with aerodynamic diameters below 5 µm, 3 µm and 1 µm were determined by using polynomial equations that adjusted for the passing volume cumulative distribution (built considering the drug mass collected in NGI-1–7 stages and the micro-orifice collector).

The geometric standard deviation (*GSD*), which represents the spread of an aerodynamic particle size distribution, was calculated as $(D_{84}/D_{16})^{1/2}$, where D_{84} and D_{16} represent the diameters at which 84% and 16% of the drug mass are recovered from the NGI 1–7 stages and micro-orifice collector, respectively.

2.5.7. Constrained drop surfactometer analysis

The effects of ABZ-STC and ABZ-SGC powders on the LS function were analyzed by the constrained drop surfactometer (CDS) method (BioSurface Instruments, Honolulu, HI) under the operating conditions previously described by Sørli et al [31-33]. Curosurf (porcine lung surfactant, LS) was diluted in water to achieve a final concentration of 2.5 mg/mL. For exposure experiments, a drop (10 µL) of the curosurf solution was placed on a pedestal. The drop was compressed/expanded less than 30% of its initial area, at a cycling frequency of 40 cycles/min to simulate the movements of the lung during breathing. For each experiment, a baseline (for the unexposed LS drop) was determined. The powders were continuously introduced into the chamber by a Venturi tube connected to a multidose aerosol device Turbuhaler®. The deposited doses were measured with a

quartz crystal microbalance (Vitrocell, Waldkirch, Germany) in real time. The dose was increased from 0 to approximately 11 µg of ABZ-STC and ABZ-SGC powders per mg of LS. The minimal surface tensions of the drop before and during exposure were analyzed for the whole range of doses using ADSA (Axisymmetric Drop Shape Analysis) [33]. The experiments were performed five times (N=5).

2.6. Statistical analysis

Statistical analysis was performed using multiple t-tests, using GraphPad Prism software v6.05 (GraphPad Software Inc, San Diego, Ca, USA). *p*-values lower than 0.05 were considered statistically significant. Data represent the mean value ± standard deviation. The number of repetitions of the experiments is indicated in each section of Material and methods.

3. Results and discussion

3.1. Characterization of the suspensions of ABZ with bile salts

Table 1 shows information about the particle size distributions of the raw ABZ powder and the suspensions before and after the homogenization and sonication processes. ABZ, as supplied, presented a median size of 76.31 µm. By producing a suspension of ABZ with bile salts, an important decrease in the D_{50} value of ABZ could be observed. Interestingly, the D_{50} of the initial ABZ-STC suspension was about 3 times larger than the D_{50} exhibited by the initial ABZ-SGC suspension, suggesting that SGC is more effective as surfactant than STC. A similar behavior was found for suspensions of tobramycin with STC and SGC [34].

To reduce particle size, homogenization and sonication of the dispersions were performed prior to HPH (Table 1). The homogenization process produced a 52% reduction in the D_{50} of the ABZ-STC system, while it did not change the D_{50} of ABZ-SGC suspension. On the other hand, sonication significantly reduced (around 50%) the particle size of both suspensions, obtaining D_{50} of 11.87 and 6.08 µm for the ABZ-STC

and ABZ-SGC systems, respectively. The span values, were close to or higher than 2, indicating that all the particle size distributions were dispersed before HPH process.

In order to confirm the higher capacity of SGC as surfactant, the surface tensions (ST) of water, the solutions of STC and SGC in water, and the ABZ-STC and ABZ-SGC suspensions were measured. The initial surface tension of water was 73.3 mN/m. By adding SGC, the surface tension of the solution decreased to 54.0 mN/m, whereas the addition of STC reduced the water surface tension to 63.4 mN/m. These results confirmed that SGC is more efficient at reducing the surface tension of water than STC. When the surface tension of the solutions of STC and SGC in water and the suspensions of ABZ containing SGC or STC were compared, an increase in the surface tension was observed for the ABZ-SGC suspension (64.4 mN/m), while the value remained almost unchanged for the ABZ-STC suspension (67.9 mN/m). These results suggest that the SGC is interacting strongly with the ABZ particles in suspension [35], which explains the increase in the water surface tension, while the interaction of STC with the ABZ particles is low, leading to a similar water surface tension in the ABZ suspension.

It is well known that the amidation of the carboxyl group with amino acids, such as glycine or taurine, contributes to changes in hydrophilic-lipophilic balance (HLB) of bile salts. Thus, tauroderivatives are more hydrophilic than glycoderivatives, which are more hydrophilic than the original salts [36]. Housaindokht et al.[37] synthesized nanostructured inorganic particles with various surfactants, having different HLB values and they found that particle size and PSD increased with increasing surfactant HLB values. These results are in agreement with our data, which showed that the suspension containing SGC has a significantly lower particle size than the suspension stabilized with STC (with higher HLB) during the whole process.

3.2. Influence of the HPH processing on the particle size of the nanosupensions

After homogenization and sonication, the suspensions of ABZ-SGC and ABZ-STC were processed by HPH and particle size distributions were analyzed as a function of the

applied homogenization cycles (Section 2S and Table S1, Supplementary material). After 10 homogenization cycles (considered appropriate to produce the ABZ nanosuspensions), the Z-average diameters were 454 and 490 nm for ABZ-SGC and ABZ-STC, respectively. Results from other authors showed that after HPH process, SGC was more suitable to stabilize tobramycin nanosuspensions, compared with STC, leading to nanosuspensions of lower particle size [34]. In the case of our formulations, although the particle size of the ABZ-SGC nanosuspensions tended to be smaller compared to ABZ-STC in all the homogenization cycles performed, the differences were not statistically significant.

3.3. Spray-drying process yield and outlet air temperature

The nanosuspensions were then processed by spray drying. Table 2 shows the SD yield and outlet air temperature for both systems. The outlet air temperature was approximately 70 °C, well below the degradation temperature reported for ABZ (140 °C) [38]. FT-Infrared Spectroscopy results confirmed that processing did not affect the chemical stability of the drug (Section 3.S, Supplementary material). The process yield was 50% for SD ABZ-STC and 60% for SD ABZ-SGC. The statistical analysis has shown that the differences in the yields of the formulations are not significant and that they can be considered acceptable for lab-scale driers [39].

3.4. Characterization of the SD powders

3.4.1. Particle size distribution and powder moisture

Table 2 presents the moisture content, D_{10}, D_{50}, D_{90} and span of the SD ABZ-STC and SD ABZ-SGC powders. Considering that a moisture content of 5% w/w is acceptable for inhalation powders [40], the combination of the selected operating conditions and formulations allowed the production of particles with very low water contents (< 1%). The comparison between formulations shows that the moisture content of SD ABZ-SGC is significantly lower than SD ABZ-STC powder. According to Seville et al., a reduction

in the ST decreases the moisture content of the dried particles due to the greater permeation of heat into the atomized liquid feed [8]. Our results (Section 3.1) showed that solutions and suspensions developed with SGC have lower surface tension than solutions and suspensions of STC. Thus, the lower moisture content of SD ABZ-SGC formulations compared with SD ABZ-STC can be due to the higher capacity of SGC to reduce the ST of ABZ formulations.

The SD ABZ-SGC and ABZ-STC powders also presented suitable geometric median diameters (lower than 4 μm) for pulmonary administration. The differences in the D_{50} values of the SD ABZ-SGC and SD ABZ-STC powders were not statistically significant. According to the span values, the SD ABZ-STC particle size distribution could be considered narrow, while it was slightly more disperse for the SD ABZ-SGC.

3.4.2. Morphology

The morphology of the ABZ raw material and SD powders (ABZ-STC and ABZ-SGC) was analyzed by scanning electron microscopy (SEM) (Figure 1).

As shown in Figure 1A, the ABZ raw material exhibited a laminar structure [60]. The ABZ raw material presented some particles that were much larger than those observed for the SD powders. This is in agreement with data obtained by laser diffraction for the ABZ raw material (D_{50} = 76.31 μm, Table 1). On the other hand, the SEM micrographs of the SD ABZ-STC and SD ABZ-SGC powders (Fig. 1B and 1C, respectively) suggest that the particles were agglomerates of small particles with a final size of approximately 4 μm, also in agreement with the previous laser diffraction results of the SD ABZ-STC and SD ABZ-SGC powders (D_{50} = 3.72 μm and 3.86 μm, respectively, Table 2). In addition, the SD ABZ-STC and SD ABZ-SGC particles seemed to present pores, due to the agglomeration of the nanoparticles.

3.4.3. Flow properties

A common indicator of powder flowability is the Carr's compressibility index (*CI*). The flow of ABZ raw material, SD ABZ-STC, SD ABZ-SGC and lactose was evaluated by means of the *CI*. According to USP, *CI* values higher than 30 indicate poor powder flowability and values lower than 25 indicate good flow characteristics [25]. As shown in Table 3, the *CI* of ABZ raw material was about 35%, exhibiting poor flow properties according to the USP. The SD powders also showed poor flowability properties (*CI* values of about 31% and 28% for SD ABZ-SGC and SD ABZ-STC systems, respectively).

The two main factors that generally affect powders flowability are particle shape and size. Spherical particles (> 50 μm) with smooth surfaces often flow better than rough non-spherical particles [41]. In addition, when particle size decreases, the flowability of the powder is reduced due to interparticle forces (primarily the Van der Waals attractive forces), which become larger in relation to gravitational and drag forces. Therefore, fine powders with median diameters smaller than 30 μm often exhibit poor flow and a tendency to agglomerate [42]. Since particles suitable for pulmonary delivery have to be very small, they are usually cohesive. Although the SD ABZ-STC and SD ABZ-SGC particles were more rounded than the raw material, the SD formulations presented particle sizes of 3.72 μm and 3.86 μm respectively (Table 2) and the poor flowability of the tested powders was expected.

Dry powder inhalers are usually formulated as a powder mixture of coarse carrier particles [43] to improve drug particle flowability, thus improving dosing accuracy and minimizing the dose variability observed with drug formulations alone [28]. Hence, in this work the SD samples were mixed with lactose with excellent flow properties (*CI*=3.13, Table 3).

3.4.4. Porosity determination

409 The surface areas of SD ABZ-STC and SD ABZ-SGC samples were 10.8 m^2/g and 8.8
410 m^2/g, respectively. These results could be attributed to both particle size and porosity.
411 According to the pore volume distribution, the use of STC as surfactant resulted in
412 enhanced product porosity. Figure 2 shows that both SD particle systems have similar
413 pore size distributions, SD ABZ-STC has pore diameters slightly larger than SD ABZ-
414 SGC. Moreover, SD ABZ-STC has more mesopores (2–50 nm) and macropores (> 50
415 nm) than SD ABZ-SGC [44].
416 It has been reported that when suspensions are dried by SD, agglomerate-like particles
417 are formed. Typically, the transformation of the nanosuspensions into aggregates by
418 spray drying employed pharmaceutical excipients, such as polymers, sugars and
419 surfactants. They act by forming “excipient bridges”, interconnecting the nanoparticles
420 [45]. The evaporation of water from sprayed droplets produces the agglomeration of
421 particles, generating porous structures which enable further moisture evaporation through
422 pores and capillaries [46]. These data agree with our analysis of surface area
423 determination (Figure 2) and with the micrographs (Figure 1), where some pores are
424 visible between the agglomerated crystals in both formulations. Moreover, these results
425 are in accordance with the low moisture levels in the obtained products (Table 2).
426 The differences in porosity found in SD ABZ-STC and SD ABZ-SGC formulations
427 could be attributed to the interaction between ABZ and the surfactants used. In this
428 sense, based on the surface tension results (see Section 3.1), we concluded that SGC
429 showed higher interaction with the suspended ABZ particles than STC. Therefore, SGC
430 could generate more interparticle bridges, which would increase the nanoparticle
431 proximity; and thus, it would decrease the porosity of the final microparticles.
432
433 *3.4.5. Aerosolization performance*
434 In order to analyze the quality of SD ABZ-STC and SD ABZ-SGC for pulmonary
435 application, the aerosolization performance of the particle systems was evaluated by
436 using the NGI cascade impactor.

Several articles have demonstrated the effects of STC and SGC as enhancers of the absorption of hydrophobic drugs and peptides-proteins, both through the pulmonary route [17] and other routes of drug administration [18, 47-51]. However, to date, the capability of the bile salts as enhancers of the aerosolization properties has not been exhaustively explored. Li et al. [15] found that if STC was incorporated into non-viral gene therapy formulations prior to SD of the solutions, this resulted in a powder with cavities, with reduced deposition in the throat and stage 1 in the evaluation of *in vitro* deposition of dry powders. The results showed that STC improved the aerodynamic properties by deaggregation of the powder agglomerates [15].

Our results for different SD powder:lactose ratios showed that the EFs were above 90% for both SD powders (Table 4). On the other hand, the FPF and RF were significantly higher for SD ABZ-STC than for SD ABZ-SGC. According to these results, the performance of SD ABZ-STC was better than that of SD ABZ-SGC, which is consistent with the data previously reported. Porous particles contain a high void space, producing particles with low density, leading to a low aerodynamic diameter, and consequently, high respiratory fractions [52]. As shown in Figure 2, the SD ABZ-STC presented higher porosity than SD ABZ-SGC, which may explain the differences in the percentages of respiratory fraction of each formulation.

For a SD powder:lactose ratio of 1:2, the *MMAD* for SD ABZ-STC was about 1.9 μm, whereas the *MMAD* for SD ABZ-SGC was about 2.3 μm (Table 5). The differences between the *MMAD* values of both formulations were not statistically significant, but a tendency to lower *MMAD* for the SD ABZ-STC, compared to SD ABZ-SGC, was found.

In order to administer a suitable drug dose by the pulmonary route, without significantly decreasing the flow properties, a SD powder-lactose ratio of 1:1 was used. The EF, FPF and RF values (Table 4) and the percentage of particles smaller than 5 μm and 3 μm (Table 5) for both formulations were similar to that obtained with a SD powder:lactose ratio of 1:2. Present results allow us to conclude that the incorporation of a high dose of

SD powder does not affect the aerodynamic behavior, and it would be a good approach for the administration of an effective dose of ABZ.

For both SD powders and different powder:lactose ratios, the RF values were higher than 70% (Table 4), and 90% of the particles presented an aerodynamic diameter below 5 µm (Table 5). The GSD values obtained (lower than 3) showed that the aerodynamic diameter distributions were narrow [53]. Therefore, the formulations could be adequately deposited throughout all the regions of the lungs and effectively reach the lower airways [54].

3.4.6. Aerodynamic behavior under special conditions

Dyspnea is a frequent symptom in patients with pulmonary CE [4, 55]. In order to determine the performances of the SD ABZ-SGC and SD ABZ-STC powders under conditions that simulate reduced respiratory capacity, cascade impactor experiments were performed using a low pressure drop of 2 KPa (Section 2.5.6).

As shown in Table 4, the RF of SD ABZ-STC:lactose (1:1) and SD ABZ-SGC:lactose (1:1) formulations were of 69.00% and 48.98%, respectively (percentages lower than RF values obtained under normal respiratory conditions). In addition, *MMAD* values and the percentage of particles smaller than 5 µm were similar to those obtained under normal conditions (Table 5). Even though the special conditions affected some aerodynamic parameters, all the values obtained are adequate for ABZ administration by inhalation. On the other hand, in agreement with our previous result under normal pressure drop (Section 3.4.5), the RF of SD ABZ-STC was significantly higher than SD ABZ-SGC. Again, it can be attributed to the higher porosity of SD ABZ-STC than SD ABZ-SGC [52].

3.4.7. Effects of ABZ dry powders on LS function

LS plays an important role in ensuring lung functionality [56]. The analysis of the minimum surface tension is a useful tool to study LS damage, given that a significant

increase in this parameter is indicative of deterioration in the surface film and could lead to alveolar collapse. It has been proposed that, if the *in vivo* minimum surface tension exceeds 10 mN/m, this may lead to atelectasis [57].

In this work, the effects of the SD ABZ-STC and SD ABZ-SGC formulations on LS functionality were studied by constrained drop surfactometer (CDS). Sørli et al. analyzed the applicability of the CDS *in vitro* model as a predictor for lung toxicity *in vivo* both for impregnation products and for potential pharmaceutical enhancers (bile salts, including the two used in the present study) [31, 58]. For impregnation products the *in vitro - in vivo* correlation demonstrated that all the analyzed products that induced acute respiration toxicity in mice upon inhalation also inhibited the LS function *in vitro*. Therefore, they concluded that this method may greatly reduce the number of animals used for toxicity testing and formulation of new products [58]. The bile salts induced rapid shallow breathing upon inhalation by mice, the concentration that induced rapid shallow breathing was ranked, and this rank was the same as when compared to the concentration that inhibited LS function [31] . The bile salt concentrations tested in the paper by Sørli et al (2018) was much higher than in the present work.

Figure 3 shows that when the SD ABZ-STC and SD ABZ-SGC powders were aerosolized and introduced into the CDS chamber, the minimum surface tension increased slightly compared to the baseline values, but they were all well below 10 mN/m. Neither formulation affected the LS function at the analyzed doses, which suggests that the SD powders do not disrupt the LS function.

4. Conclusions

In the present work, two formulations containing the hydrophobic drug ABZ and the bile salts STC and SGC, for local delivery of ABZ through the pulmonary route, were developed and compared. Both products were obtained by processing aqueous suspensions using simple and scalable techniques, such as high-pressure homogenization and spray drying. Thereby, the use of organic solvents was avoided.

Our results demonstrate that although SGC is a better suspension stabilizer than STC, the formulation containing STC presented a better aerodynamic behavior, as a result of the higher porosity of the powder, compared with SD ABZ-SGC. Thus, we conclude that the bile salt type can differently affect the porosity of the nanoaggregates obtained, leading to formulations with different aerodynamic profiles, which is relevant for lung drug delivery applications.

Nevertheless, both SD powders presented high yields, low moisture content and high percentages of respirable fraction (under normal and special conditions) and they did not affect the lung surfactant functionality. Thus, both formulations could be attractive strategies to target ABZ for the treatment of parasitic diseases affecting the respiratory system. However, drug dissolution and *in vivo* studies should be performed to establish a correlation between the *in vitro* results obtained in this work and the efficacy of the formulations.

Conflicts of interest

The authors report no conflicts of interest.

Acknowledgments

Secretaría General de Ciencia y Tecnología, Universidad Nacional del Sur (PGI 24/B252), Consejo Nacional de Investigaciones Científicas y Técnicas (CONICET, PIP 11220150100704CO), and Agencia Nacional de Promoción Científica y Tecnológica (ANPCyT, PICT-2016-0976.) support this study. Dr. Natalini and Razuc thank CONICET for their postdoctoral fellowships. The authors thank BSC Pharm. W. Starkloff (UNS), Dr. M. Piqueras, Lic. F. Cabrera (PLAPIQUI) and BSC Pharm. R. Pereyra (UNS) for their technical assistance and Plastiape (Italy) for the donation of RS01 high resistance inhalers.

References

[1] C.M. Budke, P. Deplazes, P.R. Torgerson, Global socioeconomic impact of cystic echinococcosis, Emerging infectious diseases, 12 (2006) 296-303.

[2] G. Grosso, S. Gruttadauria, A. Biondi, S. Marventano, A. Mistretta, Worldwide epidemiology of liver hydatidosis including the Mediterranean area, World journal of gastroenterology: WJG, 18 (2012) 1425-1437.

[3] M.S. Boudaya, J. Mohamed, A. Berraies, H. Zribi, A. Marghli, T. Kilani, Brief original scientific report: a new surgical approach for the treatment of left pulmonary and hepatic hydatid disease, Surgery today, 44 (2014) 1971-1974.

[4] Enfermedades infecciosas. hidatidosis. Diagnóstico de Hidatidosis. Guia para el equipo de salud, Ministerio de salud de la nacion, Buenos Aires, Argentina, 2012.

[5] F. Lötsch, J. Naderer, T. Skuhala, M. Groger, H. Auer, K. Kaczirek, F. Waneck, M. Ramharter, Intra-cystic concentrations of albendazole-sulphoxide in human cystic echinococcosis: a systematic review and analysis of individual patient data, Parasitology research, 115 (2016) 2995-3001.

[6] G. Cook, Use of benzimidazole chemotherapy in human helminthiases: indications and efficacy, Parasitology Today, 6 (1990) 133-136.

[7] T.T. Cong, V. Faivre, T.T. Nguyen, H. Heras, F. Pirot, N. Walchshofer, M.-E. Sarciron, F. Falson, Study on the hydatid cyst membrane: permeation of model molecules and interactions with drug-loaded nanoparticles, International journal of pharmaceutics, 353 (2008) 223-232.

[8] P.C. Seville, H.-y. Li, T.P. Learoyd, Spray-dried powders for pulmonary drug delivery, Critical Reviews™ in Therapeutic Drug Carrier Systems, 24 (2007) 307-360.

[9] A.H. Chow, H.H. Tong, P. Chattopadhyay, B.Y. Shekunov, Particle engineering for pulmonary drug delivery, Pharmaceutical research, 24 (2007) 411-437.

[10] A. Clark, Medical aerosol inhalers: past, present, and future, Aerosol science and technology, 22 (1995) 374-391.

[11] A. Hidalgo, A. Cruz, J. Perez-Gil, Pulmonary surfactant and nanocarriers: Toxicity versus combined nanomedical applications, Biochimica et Biophysica Acta-Biomembranes, 1859 (2017) 1740-1748.

[12] M. Razuc, J. Pina, M.V. Ramirez-Rigo, Optimization of Ciprofloxacin Hydrochloride Spray-Dried Microparticles for Pulmonary Delivery Using Design of Experiments, AAPS PharmSciTech, 19 (2018) 3085-3096.

[13] L. Gallo, M.V. Ramírez-Rigo, V. Bucalá, Development of porous spray-dried inhalable particles using an organic solvent-free technique, Powder Technology, 342 (2019) 642-652.

[14] J.O. Morales, J.I. Peters, R.O. Williams, Surfactants: their critical role in enhancing drug delivery to the lungs, Therapeutic Delivery, 2 (2011) 623-641.

[15] H.Y. Li, P.C. Seville, I. Williamson, J.C. Birchall, The use of absorption enhancers to enhance the dispersibility of spray-dried powders for pulmonary gene therapy, The journal of gene medicine, 7 (2005) 1035-1043.

[16] L. Heinemann, W. Klappoth, K. Rave, B. Hompesch, R. Linkeschowa, T. Heise, Intra-individual variability of the metabolic effect of inhaled insulin together with an absorption enhancer, Diabetes Care, 23 (2000) 1343-1347.

[17] F. Johansson, E. Hjertberg, S. Eirefelt, A. Tronde, U.H. Bengtsson, Mechanisms for absorption enhancement of inhaled insulin by sodium taurocholate, European journal of pharmaceutical sciences, 17 (2002) 63-71.

[18] F. Komada, S. Iwakawa, N. Yamamoto, H. Sakakibara, K. Okumura, Intratracheal delivery of peptide and protein agents: absorption from solution and dry powder by rat lung, Journal of pharmaceutical sciences, 83 (1994) 863-867.

[19] M.S. Mesiha, S. Ponnapula, F. Plakogiannis, Oral absorption of insulin encapsulated in artificial chyles of bile salts, palmitic acid and α-tocopherol dispersions, International journal of pharmaceutics, 249 (2002) 1-5.

[20] K. Morimoto, Y. Uehara, K. Iwanaga, M. Kakemi, Effects of sodium glycocholate and protease inhibitors on permeability of TRH and insulin across rabbit trachea, Pharmaceutica Acta Helvetiae, 74 (2000) 411-415.

[21] A. Yamamoto, S. Okumura, Y. Fukuda, M. Fukui, K. Takahashi, S. Muranishi, Improvement of the pulmonary absorption of (Asu1, 7)-eel calcitonin by various absorption enhancers and their pulmonary toxicity in rats, Journal of pharmaceutical sciences, 86 (1997) 1144-1147.

[22] E. Fröhlich, A. Mercuri, S. Wu, S. Salar-Behzadi, Measurements of deposition, lung surface area and lung fluid for simulation of inhaled compounds, Frontiers in pharmacology, 7 (2016) 1-10.

[23] F. Palazzo, S. Giovagnoli, A. Schoubben, P. Blasi, C. Rossi, M. Ricci, Development of a spray-drying method for the formulation of respirable microparticles containing ofloxacin–palladium complex, International journal of pharmaceutics, 440 (2013) 273-282.

[24] N.E. Ceschan, V. Bucalá, M.V. Ramírez-Rigo, New alginic acid–atenolol microparticles for inhalatory drug targeting, Materials Science and Engineering: C, 41 (2014) 255-266.

[25] M. Rockville, United States of Pharmacopeia-National Formulary, USP30-NF25, The United States Pharmacoepial Convention (2007) 635-645.

[26] N.E. Ceschan, V. Bucalá, M.V. Ramírez-Rigo, H.D.C. Smyth, Impact of feed counterion addition and cyclone type on aerodynamic behavior of alginic-atenolol microparticles produced by spray drying, European Journal of Pharmaceutics and Biopharmaceutics, 109 (2016) 72-80.

[27] Coplay-Scientific, Quality solutions for Who are Coplay, Edition Brochure, (2012).

[28] H. Schiavone, S. Palakodaty, A. Clark, P. York, S.T. Tzannis, Evaluation of SCF-engineered particle-based lactose blends in passive dry powder inhalers, International journal of pharmaceutics, 281 (2004) 55-66.

[29] V.A. Marple, B.A. Olson, K. Santhanakrishnan, J.P. Mitchell, S.C. Murray, B.L. Hudson-Curtis, Next generation pharmaceutical impactor (a new impactor for pharmaceutical inhaler testing). Part II: Archival calibration, Journal of Aerosol medicine, 16 (2003) 301-324.

[30] L. Gallo, V. Bucalá, M.V. Ramírez-Rigo, Formulation and characterization of polysaccharide microparticles for pulmonary delivery of sodium cromoglycate, AAPS PharmSciTech, 18 (2017) 1634-1645.

[31] J.B. Sørli, K.B. Sivars, E. Da Silva, K.S. Hougaard, I.K. Koponen, Y.Y. Zuo, I.E. Weydahl, P.M. Åberg, R. Fransson, Bile salt enhancers for inhalation: Correlation between in vitro and in vivo lung effects, International journal of pharmaceutics, 550 (2018) 114-122.

[32] J.B. Sørli, E. Da Silva, P. Bäckman, M. Levin, B.L. Thomsen, I.K. Koponen, S.T. Larsen, A proposed in vitro method to assess effects of inhaled particles on lung surfactant function, American journal of respiratory cell and molecular biology, 54 (2016) 306-311.

[33] R.P. Valle, T. Wu, Y.Y. Zuo, Biophysical influence of airborne carbon nanomaterials on natural pulmonary surfactant, ACS nano, 9 (2015) 5413-5421.

[34] G. Pilcer, F. Vanderbist, K. Amighi, Preparation and characterization of spray-dried tobramycin powders containing nanoparticles for pulmonary delivery, International journal of pharmaceutics, 365 (2009) 162-169.

[35] S.-i. Yasueda, K. Inada, K. Matsuhisa, H. Terayama, A. Ohtori, Evaluation of ophthalmic suspensions using surface tension, European journal of pharmaceutics and biopharmaceutics, 57 (2004) 377-382.

[36] J.M. Otero, Síntesis y caracterización de surfactantes derivados de sales biliares, éteres corona, adamantanos y cadenas hidrocarbonadas, Universidade de Santiago de Compostela, 2015.

[37] M.R. Housaindokht, A.N. Pour, Study the effect of HLB of surfactant on particle size distribution of hematite nanoparticles prepared via the reverse microemulsion, Solid State Sciences, 14 (2012) 622-625.

[38] S. Hengsawas Surasarang, J.M. Keen, S. Huang, F. Zhang, J.W. McGinity, R.O. Williams III, Hot melt extrusion versus spray drying: hot melt extrusion degrades albendazole, Drug development and industrial pharmacy, 43 (2017) 797-811.

[39] M. Islam, T. Langrish, An investigation into lactose crystallization under high temperature conditions during spray drying, Food Research International, 43 (2010) 46-56.

[40] S. Behboudi-Jobbehdar, C. Soukoulis, L. Yonekura, I. Fisk, Optimization of spray-drying process conditions for the production of maximally viable microencapsulated L. acidophilus NCIMB 701748, Drying Technology, 31 (2013) 1274-1283.

[41] D. Schulze, Powders and bulk solids, Behaviour, Characterization, Storage and Flow. Springer, (2008) 35-74.

[42] M. Krantz, H. Zhang, J. Zhu, Characterization of powder flow: Static and dynamic testing, Powder Technology, 194 (2009) 239-245.

[43] K. Iida, Y. Hayakawa, H. Okamoto, K. Danjo, H. Leuenberger, Preparation of dry powder inhalation by surface treatment of lactose carrier particles, Chemical and pharmaceutical bulletin, 51 (2003) 1-5.

[44] Y. Hattori, Y. Maitani, Folate-linked lipid-based nanoparticle for targeted gene delivery, Current Drug Delivery, 2 (2005) 243-252.

[45] W.S. Cheow, K. Hadinoto, Preparations of dry-powder therapeutic nanoparticle aerosols for inhaled drug delivery, Earozoru Kenkyu, 25 (2010) 155-165.

[46] I. Zbicinski, M. Kwapinska, Physical properties-formed during spray drying-of materials with the properties of an agglomerate, Acta Agrophysica, 2 (2003) 443–455.

[47] F. Mukaizawa, K. Taniguchi, M. Miyake, K.-i. Ogawara, M. Odomi, K. Higaki, T. Kimura, Novel oral absorption system containing polyamines and bile salts enhances drug transport via both transcellular and paracellular pathways across Caco-2 cell monolayers, International journal of pharmaceutics, 367 (2009) 103-108.

[48] J.J. Criado, M. Garcia-Moreno, R.R. Macias, J.J. Marin, M. Medarde, E. Rodriguez-Fernandez, Synthesis and characterization of sodium cis-dichlorochenodeoxycholylglycinato (O, N) platinum (II)–Cytostatic activity, BioMetals, 12 (1999) 283-290.

[49] Y. Maitani, S. Asano, S. Takahashi, M. Nakagaki, T. nagai, Permeability of insulin entrapped in liposome through the nasal mucosa of rabbits, Chemical and pharmaceutical bulletin, 40 (1992) 1569-1572.

[50] G. Fetih, M. Ibrahim, M. Amin, Design and characterization of transdermal films containing ketorolac tromethamine, International Journal of PharmTech Research, 3 (2011) 449-458.

[51] A. Yamamoto, A. Luo, S. Dodda-Kashi, V. Lee, The ocular route for systemic insulin delivery in the albino rabbit, Journal of Pharmacology and Experimental Therapeutics, 249 (1989) 249-255.

[52] H.-K. Chan, Dry powder aerosol drug delivery—Opportunities for colloid and surface scientists, Colloids and Surfaces A: Physicochemical and Engineering Aspects, 284 (2006) 50-55.

[53] S.S.R. Rohani, K. Abnous, M. Tafaghodi, Preparation and characterization of spray-dried powders intended for pulmonary delivery of insulin with regard to the selection of excipients, International journal of pharmaceutics, 465 (2014) 464-478.

[54] J. Mitchell, S. Newman, H.-K. Chan, In vitro and in vivo aspects of cascade impactor tests and inhaler performance: a review, Aaps Pharmscitech, 8 (2007) 237-248.

[55] S. Arinc, A. Kosif, M. Ertugrul, H. Arpag, L. Alpay, O. Unal, O. Devran, A. Atasalihi, Evaluation of pulmonary hydatid cyst cases, International Journal of Surgery, 7 (2009) 192-195.

[56] M. Griese, Pulmonary surfactant in health and human lung diseases: state of the art, European Respiratory Journal, 13 (1999) 1455-1476.

[57] K. Tashiro, Y. Matsumoto, K. Nishizuka, K. Shibata, K. Yamamoto, M. Yamashita, T. Kobayashi, Mechanism of acute lung injury caused by inhalation of fabric protector and the effect of surfactant replacement, Intensive care medicine, 24 (1998) 55-60.

[58] J.B. Sørli, Y. Huang, E. Da Silva, J.S. Hansen, Y.Y. Zuo, M. Frederiksen, A.W. Nørgaard, N.E. Ebbehøj, S.T. Larsen, K.S. Hougaard, Prediction of acute inhalation toxicity using in vitro lung surfactant inhibition, ALTEX-Alternatives to animal experimentation, 35 (2018) 26-36.

762

763

764 **Figure captions**

765

766 **Figure 1.** Morphology of ABZ raw material (A) and the SD powders of ABZ-STC (B) and
767 ABZ-SGC (C) by scanning electron microscopy (SEM) at a magnification of 8500 X and 20000
768 X.

769

770 **Figure 2.** Barrett-Joyner-Halenda (BJH) pore size distribution from N_2 adsorption isotherm
771 expressed as pore volume.

772

773 **Figure 3.** Minimum surface tension of the lung surfactant (LS) after administration of the spray
774 drying products ABZ-SGC (A) and ABZ-STC (B) at doses between 1 and 11 ug/mg of LS. Data
775 represent the mean value ± standard deviation. The experiments were performed five times
776 (n=5).

777

Table 1. Median volumetric diameter (D_{50}) and distribution width (*Span*) of ABZ-STC and ABZ-SGC suspensions (initial suspensions and suspensions obtained after homogenization and sonication operations).

	Raw material	Suspension ABZ-STC			Suspension ABZ-SGC		
Particles size	**ABZ**	**Initial suspension**	**Homogenization**	**Homogenization/ Sonication**	**Initial Suspension**	**Homogenization**	**Homogenization/ Sonication**
D_{50} **(µm)**	76.31 ± 2.99	44.97 ± 1.55	21.65 ± 0.16	11.87 ± 0.79	14.90 ± 0.12 (**)	15.57 ± 0.25 (**)	6.08 ± 0.00 (**)
Span	11.4	1.95	2.52	2.28	4.51	4.31	2.53

Asterisks (*) indicate significant differences between D_{50} values of ABZ-STC and ABZ-SGC suspensions at each stage of the process. **, $p < 0.01$.

Table 2. Particle size (D_{10}, D_{50} and D_{90}), outlet temperature, yield and moisture of SD ABZ-STC and SD ABZ-SGC powders.

	Yield (%)	**Oulet temperature (° C)**	**Moisture (%)**	D_{10} **(µm)**	D_{50} **(µm)**	D_{90} **(µm)**	***Span***
ABZ-STC	50 ± 10	68 ± 1	0.70 ± 0.04	1.10 ± 0.09	3.72 ± 0.06	8.38 ± 0.40	1.96
ABZ-SGC	60 ± 6	69 ± 1	0.56 ± 0.02 (*)	1.06 ± 0.02	3.86 ± 0.30	9.56 ± 0.80	2.20

Asterisk (*) indicate significant differences between moisture values of ABZ-STC and ABZ-SGC SD powders. *, $p < 0.05$.

Table 3. Bulk density, Tap density and Carr Index determinations of ABZ raw material, SD powders and lactose.

Material	**ABZ raw material**	**ABZ-STC**	**ABZ-SGC**	**Lactose**
δ_{bulk} **(g/mL)**	0.34 ± 0.01	0.28 ± 0.01	0.27 ± 0.00	0.66 ± 0.00
δ_{tap} **(g/mL)**	0.53 ± 0.02	0.38 ± 0.01	0.40 ± 0.01	0.68 ± 0.01
Carr Index	35.43 ± 1.54	27.61 ± 0.83	31.00 ± 1.41	3.13 ± 1.48
Flow (Classification)	Poor	Poor	Poor	Excellent

Table 4. Emitted fraction (EF), fine particle fraction (FPF) and respirable fraction (RF) of SD ABZ-STC and SD ABZ-SGC powders under different operating conditions.

	SD/Lactose ratio	Pressure drop (Kpa)	EF (%)	FPF (%)	RF (%)
ABS-STC	1:2	4	94.13 ± 1.46	83.40 ± 5.36 (*)	78.45 ± 3.83
	1:1	4	96.80 ± 2.40	79.90 ± 0.71 (*)	77.10 ± 1.06 (**)
	1:1	2	93.27 ± 2.41	73.95 ± 2.55 (**) (#)	69.00 ± 4.15 (**)(#)
ABZ-SGC	1:2	4	96.50 ± 0.51	74.20 ± 1.44	70.50 ± 3.45
	1:1	4	93.50 ± 1.08	76.50 ± 1.57	71.50 ± 2.29
	1:1	2	90.75 ± 0.78	53.97 ± 3.72 (###)	48.98 ± 2.94 (###)

Asterisks (*) indicate significant differences of FPF-RF values from SD ABZ-STC and ABZ-SGC, when comparing the same experimental conditions. Hashtags (#) indicate significant differences of FPF-RF values obtained when comparing the pressure drops of 4 kpa and 2 kpa, for each formulation. One symbol indicates $p < 0.05$; two symbols indicate $p < 0.01$ and three symbols indicate $p < 0.001$.

Table 5. Aerodynamic diameter (D_{10}, D_{50}, D_{90} and D_{99}), GSD and percentage of particles whose size are lower than 5 µm, 3 µm and 1 µm of SD ABZ-STC and SD ABZ-SGC powders.

	SD/Lactose ratio	Pressure drop (Kpa)	D_{10} (µm)	D_{50} (µm)	D_{90} (µm)	D_{99} (µm)	Particles < 5 µm (%)	Particles < 3 µm (%)	Particles < 1 µm (%)	GSD
ABS-STC	1:2	4	0.65 ± 0.03	1.87 ± 0.20	4.05 ± 0.09	8.00 ± 0.84	91 ± 3	75 ± 4	23 ± 2	2.13 ± 0.04
	1:1	4	0.80 ± 0.01	2.21 ± 0.01	4.35 ± 0.06	8.02 ± 0.01	89 ± 1	67 ± 3	10 ± 1	1.99 ± 0.01
	1:1	2	0.76 ± 0.00	2.07 ± 0.01	4.07 ± 0.07	4.89 ± 0.15	92 ± 1	74 ± 1	10 ± 1	1.98 ± 0.01
ABZ-SGC	1:2	4	0.77 ± 0.06	2.25 ± 0.14	4.56 ± 0.33	7.92 ± 0.07	90 ± 1	64 ± 6	13 ± 1	2.05 ± 0.03
	1:1	4	0.77 ± 0.02	2.21 ± 0.05	4.46 ± 0.11	7.89 ± 0.01	89 ± 2	65 ± 3	10 ± 1	2.03 ± 0.00
	1:1	2	0.75 ± 0.04	2.20 ± 0.16	4.96 ± 0.51	6.59 ± 0.04	85 ± 4	65 ± 2	12 ± 1	2.15 ± 0.04

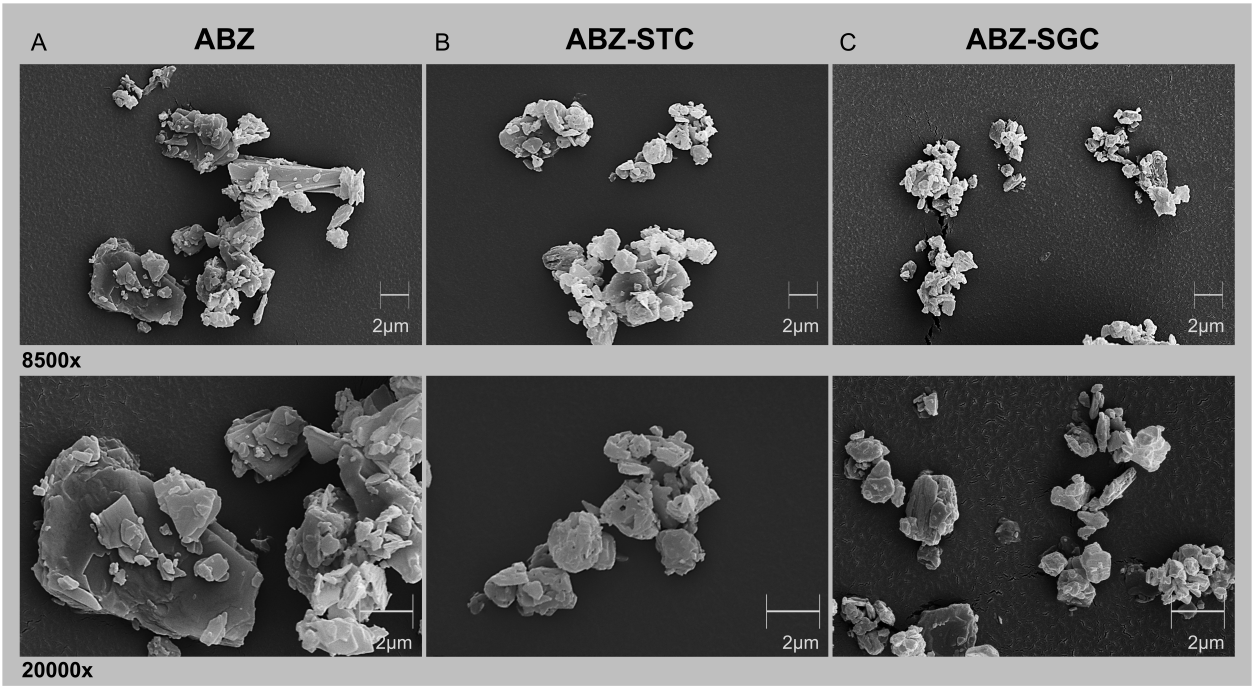

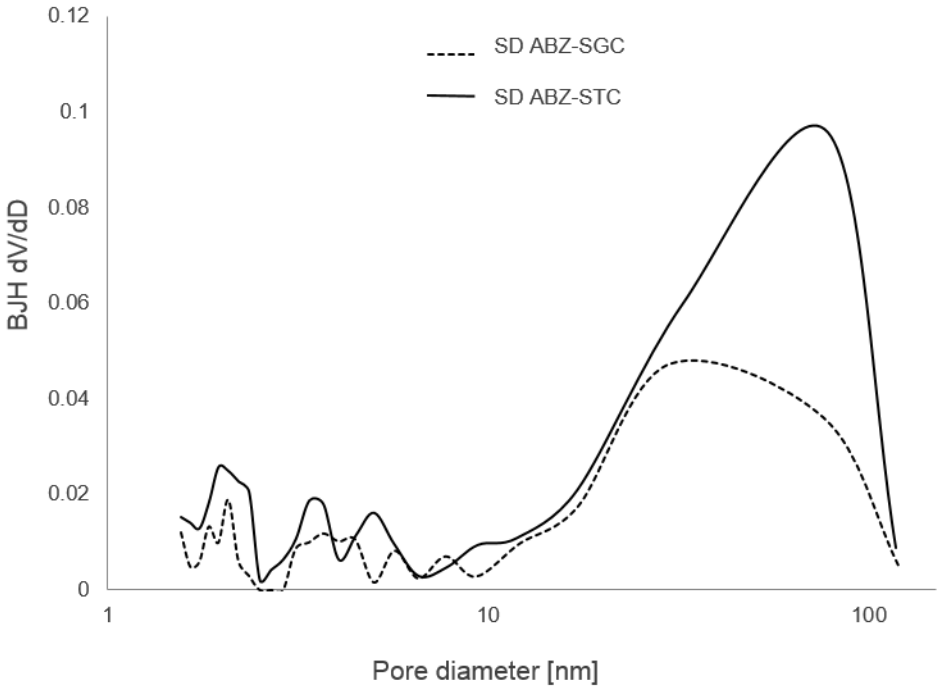

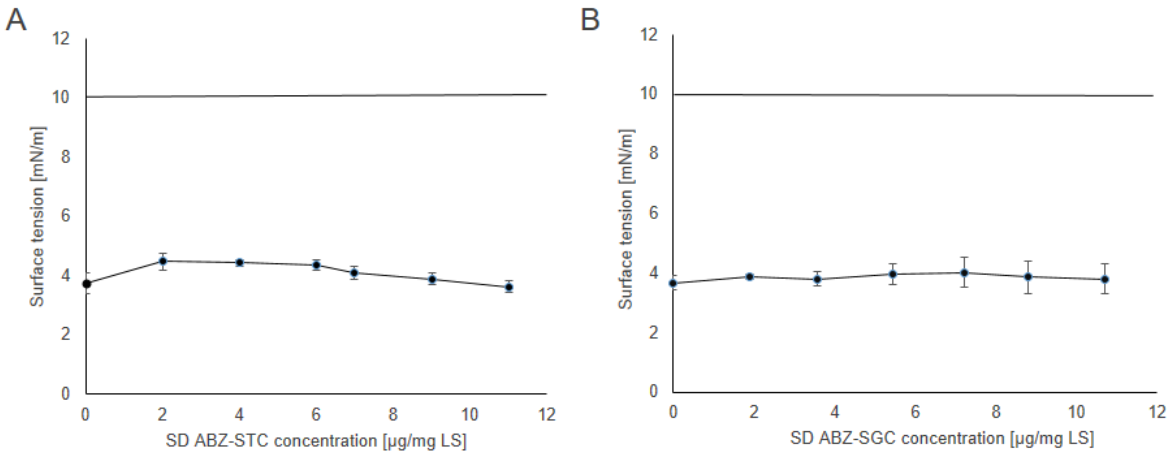
A
Surface tension [mN/m]
SD ABZ-STC concentration [µg/mg LS]
B
Surface tension [mN/m]
SD ABZ-SGC concentration [µg/mg LS]